

Near-infrared Fourier transform photoluminescence spectrometer with tunable excitation for the study of single-walled carbon nanotubes

Timothy J. McDonald

Center for Basic Sciences, National Renewable Energy Laboratory, Golden, Colorado 80401 and Department of Applied Physics, Columbia University, New York, New York 10027

Marcus Jones, Chaiwat Engtrakul, Randy J. Ellingson,
Garry Rumbles, and Michael J. Heben

Center for Basic Sciences, National Renewable Energy Laboratory, Golden, Colorado 80401

(Received 20 January 2006; accepted 23 March 2006; published online 19 May 2006)

A fast, sensitive, automated Fourier transform (FT) photoluminescence (PL) spectrometer with tunable excitation has been developed for analyzing carbon nanotube suspensions over a wide spectral range. A commercially available spectrometer was modified by the addition of a tunable excitation source, custom collection optics, and computer software to provide control and automated data collection. The apparatus enables excitation from 400 to 1100 nm and detection from 825 to 1700 nm, permitting the analysis of virtually all semiconducting single-walled nanotubes (SWNTs), including those produced by the high pressure carbon monoxide conversion and laser processes. The FT approach provides an excellent combination of high sensitivity and fast measurement. The speed advantage exists because the entire emission spectrum is collected simultaneously, while the sensitivity advantage stems from the high optical throughput. The high sensitivity is demonstrated in the measurement of very dilute SWNT suspensions and the observation of novel spectral features, and the speed is demonstrated by measuring the real-time changes in the SWNT PL during rebundling. This contribution describes the assembly of components, the methods for automating data collection, and the procedures for correcting the wavelength-dependent excitation intensity and the interferometer and detector responses. © 2006 American Institute of Physics. [DOI: 10.1063/1.2198748]

The study of single-walled carbon nanotube (SWNT) optical properties has emerged as a major area of interest. The optical properties of nanotubes are of interest from a fundamental point of view,¹⁻³ for possible photonic applications,⁴⁻⁷ and as a method for determining composition and quality of SWNT distributions.⁸⁻¹¹ Current SWNT synthesis methods produce distributions of metallic and semiconducting nanotube species. The tubes within these distributions have optical properties that are dependent on the diameter and chirality of each type of tube.¹² Semiconducting SWNTs have a gap in the electronic density of states and sharp optical transitions associated with van Hove singularities. The lowest-energy transition between the first set of van Hove singularities is typically in the near-infrared (NIR) portion of the optical spectrum,¹³ while the second and third optical transitions lie at higher energy, in the visible and ultraviolet regions of the spectrum, respectively.³ Surfactant-stabilized aqueous suspensions of SWNTs have recently shown photoluminescence (PL) from the transition associated with the first van Hove transition after excitation of higher lying transitions.¹ Since different nanotube species differ in band structure, photoluminescence excitation spectroscopy (PLE), which maps PL intensity as a function of excitation and emission energy, can be used to uniquely identify the tubes present in a sample. Consequently, PLE has emerged as an important tool for SWNT characterization.⁹

Kataura *et al.*¹³ performed the first optical absorption measurements on a collection of SWNTs and identified semi-

conducting and metallic nanotube optical transitions. Soon thereafter O'Connell *et al.*¹ measured PL emission from SWNTs suspended by aqueous surfactants. PLE measurements were subsequently performed by Bachilo *et al.*⁹ in which a grating spectrometer was used for emission detection. The promise of Fourier transform (FT) spectroscopy with a tunable excitation in the study of SWNT optical transitions was first demonstrated by Lebedkin *et al.*¹⁰

The observed PL quantum efficiency for SWNT suspensions is only $\sim 10^{-3}$,^{1,2,14} and many processing and purification procedures result in low concentrations of emissive nanotubes. It is therefore important to be able to detect weak emission in the NIR with a high signal-to-noise ratio. The advantages of FT spectroscopy in the NIR make this system ideal for collection of such emission. Also, for nanotube spectroscopy, it is desirable that the excitation source be continuously tunable across the full visible range of the optical spectrum. Such flexibility is necessary for mapping out the complete PLE spectrum, for imaging excitonic structure,² and for probing charge and energy transfer phenomena between nanotubes and other species.

This contribution extends beyond the work of Lebedkin *et al.*¹⁰ by describing in detail the construction and capabilities of a fully optimized FT-PLE system for nanotube spectroscopy. No commercial FT-based NIR fluorimeter with tunable excitation is currently available. We describe the optimization of the excitation source and the collection optics, the methods for correcting the wavelength-dependent

excitation intensity and spectrometer response, and the computer methods for operating this fast, sensitive FT-PLE apparatus. We show the advantages of this apparatus through the range of nanotube species that it is able to detect, the speed of data collection, and the sensitivity to low-concentration SWNT suspensions.

A Fourier transform spectrometer utilizes a two-beam interferometer to measure the spectral characteristics of light coming from a sample. A semireflective window divides the emitted light into two paths, each with approximately equal intensity. One path is terminated with a fixed retromirror, while the second path is varied in length by controlled movement of another retromirror. The two beams converge and the resulting intensity is measured. Spectral components within the two interfering beams may recombine constructively or destructively depending on the difference in the path lengths. The interference fringe intensity versus the moving mirror position, as measured by a detector, is the Fourier transform conjugate of the detected light spectrum.¹⁵ The inverse Fourier transform of the interferogram yields the detected spectrum for the measured frequencies in only one cycle of the moving mirror. Slower mirror speeds result in longer integration and acquisition times but yield reduced noise. The interferogram may also be averaged over several scans to reduce noise.

It is important to note that the FT spectrometer offers fundamental advantages over grating spectrometers in the PLE spectroscopy of nanotubes. Since all wavelengths are measured simultaneously, more averaging can be done in a given period of time, resulting in an increase in the signal-to-noise ratio versus single-channel detection spectrometers through the so-called Fellgett or multiplex advantage.^{15,16} Grating-based charge-coupled device and diode array detection also utilize the multiplex advantage, but gratings have limited spectral resolution in the NIR and, therefore, must be used in conjunction with slits to achieve acceptable resolution.¹⁷ Unfortunately, slits limit the amount of the emission beam that can be measured and a substantial throughput penalty is incurred. The large circular aperture of the interferometer allows for more optical throughput than is possible through the slits of a monochromator, giving rise to what is known as the Jacquinot advantage.^{18,19} Furthermore, because wavelength measurements are referenced to an internal laser, the need for spectral calibration is eliminated (Connes advantage²⁰).

Despite the fact that no commercial FT-based NIR fluorimeters with tunable excitation are available, a straightforward customization of a commercially available FT-Raman system allows for the development of the FT-PLE apparatus. We utilized a Thermo-Nicolet FT960 Raman spectrometer that contains a 1064 nm diode laser for excitation and a liquid nitrogen cooled germanium detector for measuring sample emission from 825 to 1700 nm. The FT960 has two 1064 nm holographic notch filters to remove excitation light from entering the detector chamber and, as a first step in converting the FT960 to a FT-PLE spectrometer, these two filters must be removed to permit a custom excitation source to be used. One filter is located in the window between the sample chamber and the interferometer chamber, and the second is between the interferometer chamber and the detector chamber.

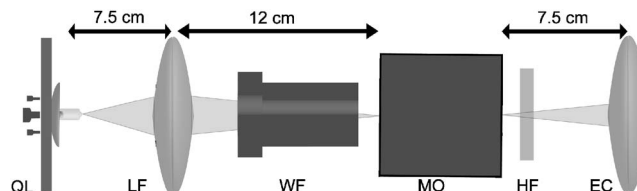


FIG. 1. FT-PLE excitation source and optics. QL: quartz tungsten halogen lamp, LF: biconvex lamp focusing lens, WF: water-filled filter, MO: single-grating monochromator, HF: optional heat-absorbing filter, and EC: biconvex excitation collimating lens.

To couple light effectively into the transitions associated with the second van Hove singularities in the density of states (DOS) of the SWNTs, the excitation source needs to be intense in the visible to NIR range of the spectrum. A 250 W quartz tungsten halogen lamp (Newport model 6334) has emission intensity that smoothly varies across this region. The lamp is powered by a stable dc power supply (HP model 6264B), and the supply voltage can be adjusted to change the temperature of the filament and the peak emission wavelength. We find that lamp life and light throughput are maximized at 22 V and 10 A, affording an average of about 10 days of continuous operation.

Figure 1 depicts the positioning of the lamp, the monochromator, and the filters and lenses associated with the tunable excitation source. The quartz lamp (Fig. 1, QL) is mounted with the filament arranged vertically to efficiently couple light into the entrance slits of the monochromator (Fig. 1, MO). A 50 mm diameter, 50 mm focal length, biconvex lens with a broadband antireflection coating (Newport model KBX142AR.16) provides lamp focusing (Fig. 1, LF) to introduce light into the 0.125 m monochromator (Acton Research Corporation, SpectraPro 275). The monochromator has an aperture ratio of $f/3.8$ and is equipped with a grating blazed at 500 nm with 600 lines/mm. Light diverging from the exit slit of the monochromator is passed through an excitation collimation lens (Fig. 1, EC), which is a 58 mm diameter, 50 mm focal length, two-element lens with a single-layer MgF₂ antireflection coating (Melles Griot model 01 CMP 117). The quartz lamp-monochromator excitation system with a monochromator bandwidth of 9 nm has a peak wavelength at 650 nm with an intensity of 1.8 mW. Since the NIR sample emission to be detected is very low in intensity, even a small amount of unwanted NIR light from the quartz lamp passed through the monochromator can interfere with the measurement. To avoid this problem, filters are employed. A 3 in. liquid filter (Newport model 6214), filled with de-ionized (DI) water (Fig. 1, WF), is inserted between the lamp focusing lens (Fig. 1, LF) and the monochromator (Fig. 1, MO) to absorb wavelengths longer than ~ 1000 nm. For solid samples, where reflection of excitation light is more of a problem, an additional heat-absorbing filter, KG2, is used (Melles Griot model 03 FCG 165) between the monochromator and the excitation collimation lens (Fig. 1, HF). Figure 2 shows the intensity distribution as a function of energy for the lamp-monochromator excitation system as determined by a thermopile detector. Figure 3 depicts the arrangement of the optics and positioners near the sample holder. Light coming from the excitation collimation lens (Fig. 3, EC) is focused to a 3 mm spot and directed onto the sample cuvette (Fig. 3, SC) with a 25 mm diameter, 38 mm

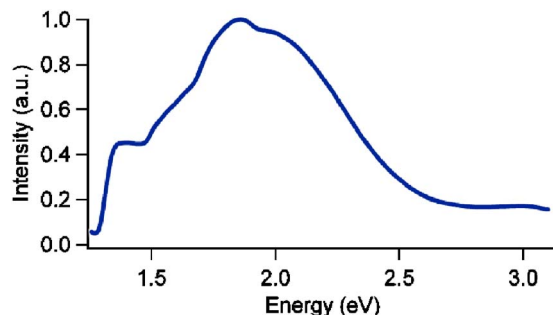


FIG. 2. (Color online) Excitation intensity profile from quartz tungsten halogen bulb coupled to single-grating monochromator with emission bandwidth of 9 nm. The intensity is recorded every 1.0 nm by a thermopile-amplifier system described in the text. The reduced intensity at low energy is due to a de-ionized water liquid filter used to remove excitation light that could scatter into the detection apparatus.

focal length biconvex lens with an AR16 coating (Newport model KBX049AR.16) [excitation focusing (EF) lens Fig. 3]. We note that all lenses are mounted on two-dimensional translation stages, and the sample holder can be rotated as well as translated.

The FT approach requires that the collected light be collimated and directed along the axis of the interferometer. Toward this end, the sample is placed at the focal point of a 75 mm diameter, 50 mm focal length aspheric collection lens with a single-layer MgF_2 antireflection coating (Fig. 3, AC) (Newport model KPA055). The HeNe laser in the apparatus is coaxial with the axis of the interferometer and useful for aligning the sample. If the sample is placed at the focal point of the laser, the sample will be very close to the optimal collection position. Since the HeNe laser can also excite the sample, a long-pass filter (Fig. 3, LP), RG 695 (Melles Griot model 03 FCG 109), is placed between the collection aspheric lens and the interferometer prior to taking a measurement. If the excitation wavelength is in the region in which the Ge detector is sensitive (>815 nm), then additional long-pass filters are required at the interferometer window (Fig. 3, IW).²¹

Data from dilute solutions of suspended nanotubes can be collected in the 90° excitation geometry shown in Fig 3.

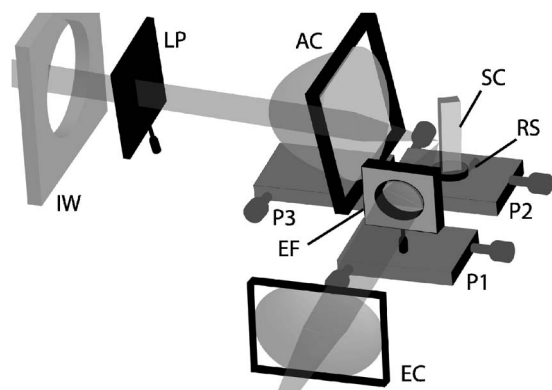


FIG. 3. Modified FT-PLS sample chamber for study of SWNT photoluminescence in the IR with a tunable excitation source. EC: excitation collimation biconvex lens, EF: excitation focusing lens, SC: sample cuvette, RS: rotation stage, P1–P3: two-dimensional translation micrometers, AC: achromatic collection lens, LP: emission long-pass filter(s), and IW: interferometer window. (Not pictured: height adjustment micrometers for AC.)

High optical density and solid samples can be analyzed by front-face illumination, where excitation and emission probe the same face of the cuvette or film. In this case the excitation beam axis and the sample face are arranged at an angle of 22.5° so reflected excitation light cannot enter the collection optics. The emission, which occurs in all directions, can still be collected with a relatively high efficiency. Facile alignment can be achieved by temporarily removing the long-pass filter to allow the HeNe laser to come to focus at the point of optimized collection. By adjusting the positioners such that the excitation light and the HeNe emission come into focus at the same point, the PL throughput can be maximized.

Thermo-Nicolet's spectrometer software, OMNIC, controls data collection for the FT960. In order to coordinately control the FT960 with the excitation light from the monochromator, LABVIEW (National Instruments, version 7.1) is used to send commands to the spectrometer's software as well as to control the monochromator. Dynamic data exchange (DDE), a Microsoft Windows interprocess communication tool, is utilized to allow a LABVIEW virtual instrument (VI) to direct the spectrometer software to take and save spectra.²² The VI interfaces with the monochromator via an RS232 connection. The VI adjusts the excitation wavelength, directs the spectrometer to collect and save emission data at that particular excitation wavelength, and repeats until data have been collected over the desired excitation range.²³

Two corrections need to be made to the collected PLE data to ensure that the measured PLE spectra represent the intrinsic properties of the nanotubes being studied. The first correction accounts for the fact that the halogen light source and monochromator system do not produce equal intensity at every excitation wavelength. To address this concern we employed a thermopile to determine the wavelength-dependent excitation intensity profile from the lamp-monochromator combination since, in contrast to diodes, thermopiles have a linear response across a wide spectral range. To improve the signal-to-noise of the thermopile, the thermopile output was preamplified with a dc-coupled amplifier (Dexter Research Center model 1010) and measured using a lock-in amplifier (Princeton Applied Research model 186A). The output from the monochromator was modulated at 13 Hz with a chopper and the in-phase component of the signal was measured with an Agilent 34401A digital multimeter. Since the monochromator is also computer controlled, the excitation intensity profile measurement can be automated for generating lamp corrections each time the halogen bulb is replaced or a new excitation filter is utilized.

The second correction accounts for the wavelength-dependent sensitivity of the interferometer and the germanium detector. To address these issues we measured a broad spectral profile from a calibrated tungsten source (Gamma Scientific RS-1) with the FT-PLS system. A diffusive plate was used to reduce the intensity of the lamp while preserving the intensity profile. The ratio of the actual to the measured spectrum was used as the wavelength-dependent response of the interferometer and Ge detector.

Figure 4 shows the PLE spectra obtained from two different SWNT dispersions prepared by previously reported methods in sodium dodecylbenzene sulfate (SDBS).^{2,24} The top panel shows data obtained with SWNTs produced by the

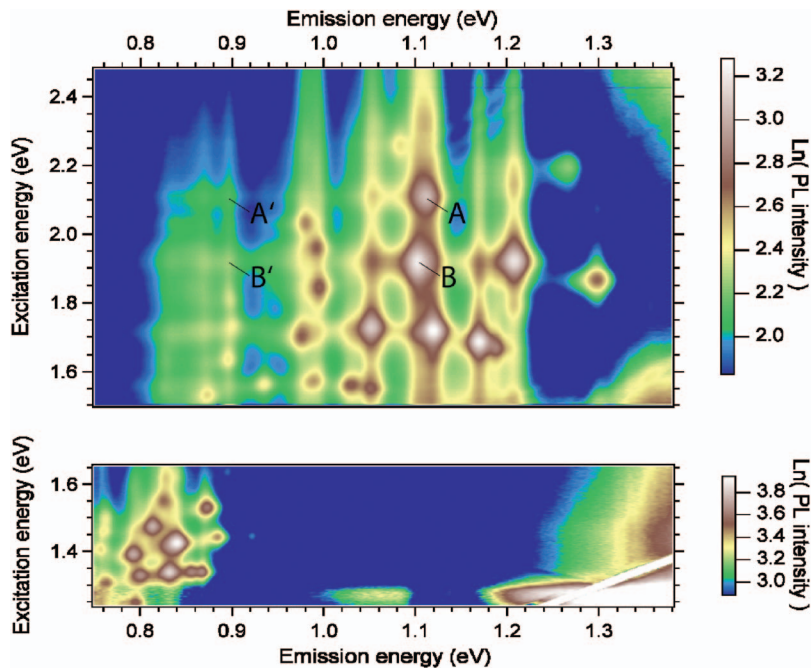


FIG. 4. (Color) Photoluminescence excitation spectra from SDBS suspensions of HiPCO (top) and PLV (bottom) SWNTs. The vertical axis is the excitation energy, and the horizontal axis is the emission energy. The emission from the sample is collected with excitation steps of 1 nm. The color is proportional to the natural logarithm of the emission intensity and is in arbitrary units. The point labeled A marks emission attributed to the (8,4) nanotube, and B marks emission from the (7,6) nanotube. Emission features at A' and B' have excitation and emission values not attributed to any SWNT band gap.

high pressure carbon monoxide conversion (HiPco) method (Carbon Nanotechnologies Inc.) in which 22 distinct semiconducting nanotubes are detected. The bottom panel of Fig. 4 shows the data for 20 unique SWNTs produced by our in-house pulse laser vaporization (PLV) technique, as previously described.^{25,26} Together, the two data sets demonstrate the capability of the FT-PLE instrument to obtain high quality data over a wide spectral range. Note that the diameter range of the SWNT structures shown in the figure spans from 7.57 to 13.77 Å, which covers the full range of SWNT types that can be synthesized or purchased commercially. Such a wide range of SWNT measurement with a single instrument has not been demonstrated previously. Also of importance is the fact that the relative excitation and emission intensities have been corrected for the wavelength-dependent excitation profile and instrument response. With the corrected data in hand one can readily compare relative quantum yields and rigorously fit the excitation and emission profiles. The emission observed around 1.3 eV in the spectrum of PLV-generated nanotubes is due to scattered excitation light, and the broad emission at energies higher than 1.3 eV in both spectra is due to the poor sensitivity and large correction factors required near the high-energy limit of the Ge detector. The diagonal features near the top of the HiPCO spectra are due to stray light leaking through the excitation monochromator. Such limitations could be readily overcome, if desired, with appropriate combinations of filters and the use of a different detector.

The previously described multiplex advantage coupled with the tunable excitation source and the available computer control enables very rapid data collection so that changes in PL emission occurring on the time scale of a few minutes can be quantified. Complete, high-resolution PLE spectra, such as those shown in Fig. 4, currently require about 5 h to be acquired. However, once the peak excitation energies at the second lowest-energy transition for specific tubes have been identified the excitation monochromator may be stepped to selectively excite only specific tubes of interest. By record-

ing the emission while exciting only at the peak energy for the nanotube species of interest, the acquisition time for an emission spectrum can be reduced to 45 s. Figure 5 shows the PL intensity and emission redshift as a function of time for a single type of nanotube [(10,2) tube in this case] in a surfactant-stabilized suspension after the surfactant concentration has been diluted below the critical micelle concentration. The time resolution permits the observation of the quenching of the nanotube emission as the statistical processing of rebundling brings metallic nanotubes into contact with semiconducting nanotubes. Also, the redshift in the emission peak indicates communication between contacting nanotubes prior to complete quenching, in agreement with other reports.^{27–31} Since SWNTs are very sensitive to their surrounding environment,³² the time-dependent PL information can reveal the kinetics of nanotube-nanotube interactions, dielectric changes in the environment, and the effects

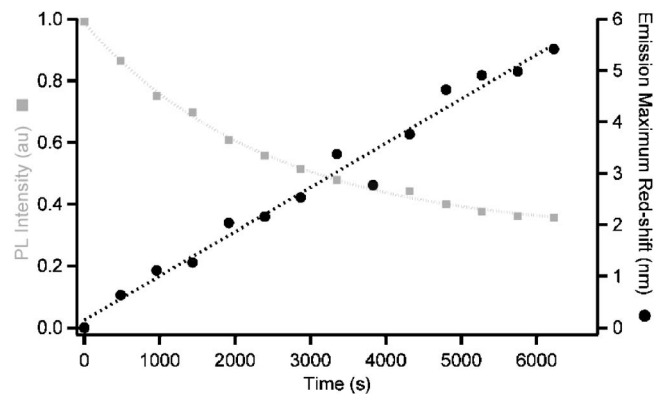


FIG. 5. PL Intensity (squares) and PL emission redshift (circles) vs time for luminescence from a single nanotube species [the (10,2) tube] in a suspension diluted below the critical micelle concentration at $t=0$. Emission spectra were recorded sequentially for seven different excitation wavelengths every 8 min for this particular experiment, but only the information extracted for emission attributed to the (10,2) nanotube via excitation at 742 nm is shown.

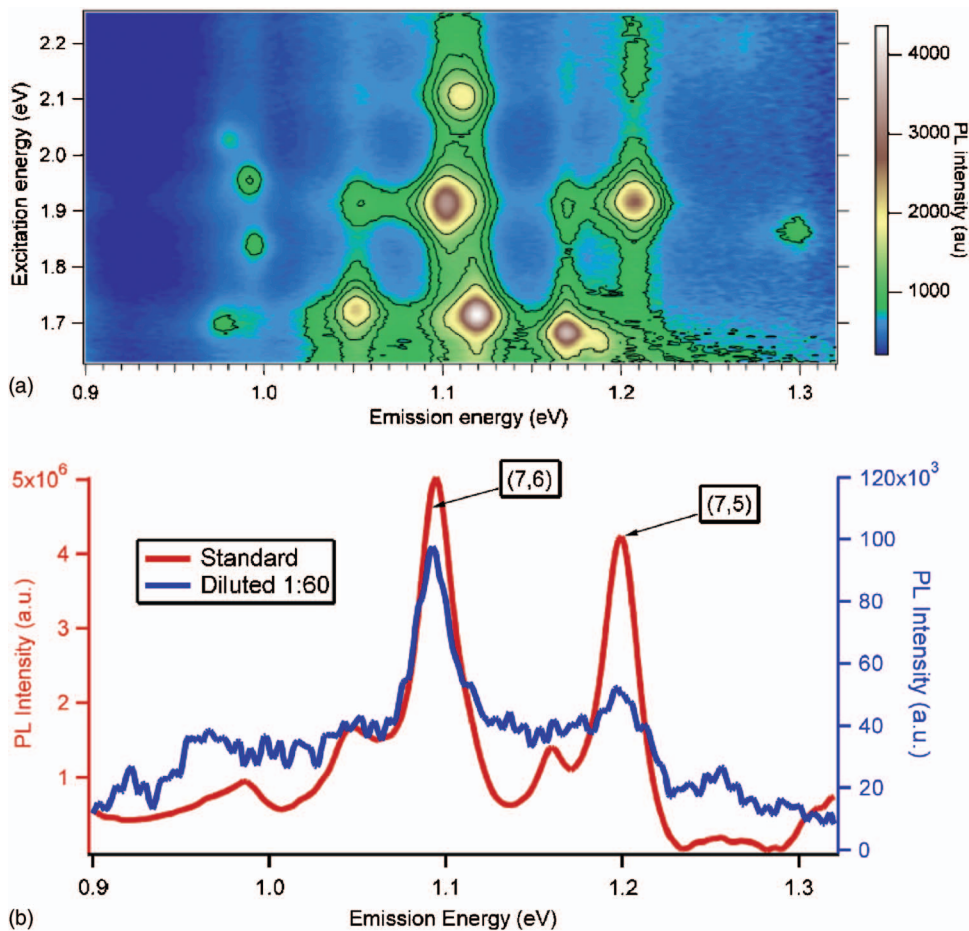


FIG. 6. (Color) (A) PLE spectra for a suspension of SWNTs at a concentration which is only 1/60 that of the standard suspension. The emission from the sample is collected with excitation steps of 1 nm. A 1% (wt/wt) aqueous solution of sodium cholate was sonicated with HiPCO SWNTs, centrifuged, and subsequently diluted with additional water and surfactant. (B) A comparison of the emission with excitation at 650 nm of the standard suspension and the diluted suspension. These spectra are cross sections from the contour maps in Fig. 4 and this figure.

of molecules introduced to the vicinity of the nanotube's surface. Such information will be valuable in future attempts to purify and separate nanotubes. Also, we note that the speed of acquisition could be significantly increased to permit observation of faster kinetic phenomena by using more intense laser excitation sources.³³ For example, the on-board 1064 nm laser diode enables PL spectra to be obtained in 1 s. In this case, the time between measurements is limited by data transfer rates that could be increased with improved software.

The system allows for the detection of PL with an excitation power of only 1–2 mW despite the fact that SWNT photoluminescence quantum yields are relatively low ($<10^{-3}$). In fact, the Jacquinot advantage and the optimized collection optics permit the measurement of PLE data from very dilute SWNT suspensions. For example, Fig. 6 shows the PLE spectra for a sample in which the SWNT concentration is only 1.7% of the concentration that is typically used.¹ Thus, the FT-PLE apparatus allows the study of suspensions that are diluted during processing efforts to, for example, separate or purify nanotubes based on length, diameter, or chirality. Being able to study low-concentration collections in real time will aid in efforts to separate SWNTs by structure and electronic character.

In addition to permitting the analysis of dilute suspensions, the sensitivity of the FT-PLE apparatus may reveal new physics. For example, the two features denoted by A' and B' in Fig. 4 are not associated with the known optical transitions for any tube which emits near 0.9 eV. One notes that the excitation energies associated with these features are

the same as the excitation maxima for the nanotubes marked by A and B, respectively. Thus, one possible explanation is that A' and B' are images in the DOS of the tube which does emit at 0.9 eV due to energy transfer from tubes at the points labeled A and B, respectively, that emit at higher energy. Energy transfer from a high band-gap to a lower band-gap nanotube has been discussed as a possible energy relaxation mechanism.³ Another possibility is that the features labeled A' and B' are due to phonon-assisted transitions in the emission from tubes that are identified by the spots at A and B, respectively. In this case, the phonon replica appears at an emission energy that is lower by the phonon energy, ~ 200 meV. Interestingly, the energy of the phonon associated with the well-known Raman G-band mode is at ~ 200 meV, and a satellite peak at an energy ~ 200 meV above the excitation maximum has been noted in other recent PLE studies.² Though the specific origin of the A' and B' peaks is presently not certain, the observation of the peaks would not be possible without the high sensitivity and large detection range available in the FT-PLE spectrometer described here.

Finally, we note that the system as described here has been optimized for a wide range of excitation wavelengths and relatively rapid measurement throughput of analysis. Several modifications could be readily made to improve specific attributes of the apparatus. For example, the monochromator bandwidth could be reduced below 9 nm in order to obtain smaller excitation step sizes and higher-resolution spectra. The increased resolution would, however, come at the expense of reduced light throughput and longer acquisi-

tion times with the currently used broadband excitation source. Of course, alterations could be made to the excitation system that would allow for more intense excitation. For example, tunable lasers could be used to provide much greater intensity over a narrow spectral range, or a xenon source could be used to provide more power in the ultraviolet portion of the spectrum. These approaches would permit much higher excitation intensity and enable high-spectral resolution measurements but would limit investigations to a smaller range of nanotube diameters. If only a small subset of nanotube types were to be studied, one could use a monochromator grating blazed for optimal performance over the particular energy region of interest.

In conclusion, we have described a FT-PLE apparatus that can quickly measure a wide range of nanotube species with high sensitivity. The fast collection allows for the measurement of PL as a function of time such that the dynamics of PL quenching and nanotube rebundling can be observed. The sensitivity allows for study of low concentration or samples of low quantum yield, and the observation of new spectroscopic features. In addition to the analysis of SWNTs, this instrument will also be useful for studying other materials or molecules that exhibit luminescence in the NIR, such as PbSe and PbS quantum dots or species involving rare-earth lanthanides.

The authors thank Jeffrey Blackburn and Anne Dillon for helpful discussions. This work was funded by the U.S. Department of Energy's Solar Photochemistry Program within the Office of Science, Office of Basic Energy Sciences, Division of Chemical Sciences, Geosciences, and Biosciences.

¹M. J. O'Connell *et al.*, *Science* **297**, 593 (2002).

²M. Jones, C. Engrakul, W. K. Metzger, R. J. Ellingson, A. J. Nozik, M. J. Heben, and G. Rumbles, *Phys. Rev. B* **71**, 115426 (2005).

³J. Jiang, R. Saito, A. Gruneis, S. G. Chou, G. G. Samsonidze, A. Jorio, G. Dresselhaus, and M. S. Dresselhaus, *Phys. Rev. B* **71**, 205420 (2005).

⁴M. S. Arnold, J. E. Sharping, S. I. Stupp, P. Kumar, and M. C. Hersam, *Nano Lett.* **3**, 1549 (2003).

⁵J. A. Misewich, R. Martel, P. Avouris, J. C. Tsang, S. Heinze, and J. Tersoff, *Science* **300**, 783 (2003).

⁶Z. C. Wu, Z. H. Chen, X. Du, *et al.*, *Science* **305**, 1273 (2004).

⁷M. Freitag, Y. Martin, J. A. Misewich, R. Martel, and P. Avouris, *Nano Lett.* **3**, 1067 (2003).

⁸S. Reich, C. Thomsen, and J. Robertson, *Phys. Rev. Lett.* **95**, 077402 (2005).

⁹S. M. Bachilo, M. S. Strano, C. Kittrell, R. H. Hauge, R. E. Smalley, and R. B. Weisman, *Science* **298**, 2361 (2002).

¹⁰S. Lebedkin, K. Arnold, F. Hennrich, R. Krupke, B. Renker, and M. M. Kappes, *New J. Phys.* **5** (2003).

¹¹Y. Miyauchi, S. Chiashi, Y. Murakami, Y. Hayashida, and S. Maruyama, *Chem. Phys. Lett.* **387**, 198 (2003).

¹²S. Iijima and T. Ichihashi, *Nature (London)* **363**, 603 (1993).

¹³H. Kataura, Y. Kumazawa, Y. Maniwa, I. Umezu, S. Suzuki, Y. Ohtsuka, and Y. Achiba, *Synth. Met.* **103**, 2555 (1999).

¹⁴F. Wang, G. Dukovic, L. E. Brus, and T. F. Heinz, *Phys. Rev. Lett.* **92**, 177401 (2004).

¹⁵P. R. Griffiths, *Transform Techniques in Chemistry* (Plenum, New York, NY, 1978).

¹⁶P. Fellgett, *J. Phys. Radium* **19**, 187 (1958).

¹⁷P. R. Griffiths, H. J. Sloane, and R. W. Hannah, *Appl. Spectrosc.* **31**, 485 (1977).

¹⁸P. Jacquinot and J. C. Dufour, *J. Rech. C. N. R. S.* **6**, 91 (1948).

¹⁹J. Barbillat, P. Le Barny, L. Divay, E. Lallier, A. Grisard, R. Van Deun, and P. Fias, *Rev. Sci. Instrum.* **74**, 4954 (2003).

²⁰J. Connes and P. Connes, *J. Opt. Soc. Am.* **56**, 896 (1966).

²¹The RG 850 filter (Melles Griot 03 FCG 118) is retained for excitation at wavelengths longer than 815 nm. Additionally, the RG 1000 filter (Melles Griot 03 FCG 113) is used for excitation wavelength beyond 850 nm, and a 1200 nm long-pass filter is used (TFI Technologies 1200LP) for excitation wavelength longer than 1000 nm.

²²In creating a DDE connection with OMNIC, the service input should be set to OMNIC and the topic input should be set to SPECTRA.

²³LABVIEW includes DDE open conversation. vi, DDE execute. vi, and DDE close conversation. vi, VIs that enable initiation of a connection, the statement for OMNIC to execute, and the termination of the connection, respectively. Source <http://zone.ni.com/devzone/devzone.nsf/webcategories/B7AA6C07A04F6A708625683C000023F6>

²⁴M. F. Islam, E. Rojas, D. M. Bergey, A. T. Johnson, and A. G. Yodh, *Nano Lett.* **3**, 269 (2003).

²⁵A. C. Dillon, T. Gennett, K. M. Jones, J. L. Alleman, P. A. Parilla, and M. J. Heben, *Adv. Mater. (Weinheim, Ger.)* **11**, 1354 (1999).

²⁶T. Gennett, A. C. Dillon, J. L. Alleman, K. M. Jones, F. S. Hasoon, and M. J. Heben, *Chem. Mater.* **12**, 599 (2000).

²⁷P. Delaney, H. J. Choi, J. Ihm, S. G. Louie, and M. L. Cohen, *Phys. Rev. B* **60**, 7899 (1999).

²⁸Y. K. Kwon, S. Saito, and D. Tomanek, *Phys. Rev. B* **58**, R13314 (1998).

²⁹P. Delaney, H. J. Choi, J. Ihm, S. G. Louie, and M. L. Cohen, *Nature (London)* **391**, 466 (1998).

³⁰M. J. O'Connell, S. Sivaram, and S. K. Doorn, *Phys. Rev. B* **69**, 235415 (2004).

³¹V. C. Moore, M. S. Strano, E. H. Haroz, R. H. Hauge, R. E. Smalley, J. Schmidt, and Y. Talmon, *Nano Lett.* **3**, 1379 (2003).

³²V. Perebeinos, J. Tersoff, and P. Avouris, *Phys. Rev. Lett.* **92**, 257402 (2004).

³³M. J. O'Connell, E. E. Eibergen, and S. K. Doorn, *Nat. Mater.* **4**, 412 (2005).